Nonlinear Analysis: Modelling and Control, Vol. 30, No. 3, 386–404
https://doi.org/10.15388/namc.2025.30.38977

Codimension-two bifurcation analysis of a discrete predator–prey system with fear effect and Allee effect*

Ceyu Lei, Xiaoling Han

Department of Mathematics, Northwest Normal University,
Lanzhou, 730070, China
hanxiaoling9@163.com

Received: June 25, 2024 / **Revised:** January 27, 2025 / **Published online:** March 3, 2025

Abstract. In this paper, we study the dynamic behavior of a discrete predator–prey model with fear effect and Allee effect by theoretical analysis and numerical simulation. Firstly, the existence and stability of the equilibrium points of the model are proved. Secondly, the existence of codimension-2 bifurcations ($1:2$, $1:3$, and $1:4$ strong resonances) in the case of two parameters is verified by bifurcation theory. In order to illustrate the complexity of the dynamic behavior of the model in the two-parameter space, we simulate the bifurcation diagrams, phase diagrams, maximum Lyapunov exponent diagrams, and isoperiodic diagram, and we verify the influence of model parameters on the population size.

Keywords: discrete model, stability, codimension-2 bifurcation, chaos.

1 Introduction

Discrete models are considered to be an important tool in the study of mathematical biology modeling. When the generations of a population do not overlap with each other, a difference equation is needed to describe it. On the other hand, the numerical simulation of continuous models is also obtained by discretizing these models. In particular, discrete models are often more accurate and convenient. In the past few decades, the dynamic behavior of discrete predator–prey systems has been extensively studied; see [1, 7, 9, 13, 14, 21, 23, 26, 29, 30] and the references therein. In 1976, May took the lead in revealing that a simple discrete model can achieve chaos through period doubling bifurcations [17]. The results showed that a simple discrete model can produce extremely complex behavior.

Studies have shown that prey fear of predators has a serious impact on the birth rate of prey [27]. In 2016, Wang et al. [24] first mathematically characterized the fear effect, that is, $F(k, y) = 1/(1 + ky)$, where $k \geqslant 0$ reflects the level of fear, which drives antipredator

*This research was supported by National Natural Science Foundation of China (No. 12161079) and Innovative Fundamental Research Group Project of Gansu Province (No. 24JRRA778).

behavior of the prey. Since then the study of the fear effect has attracted great attention. One can see literature [6, 12, 15, 20, 25].

When there are too many biological populations, resource competition might impede population growth. As a result, each population has a particular optimal growth and reproduction density, a phenomenon known as the Allee effect [22]. Empirical evidence of Allee effects has been observed in many natural species, for example, plants [8], birds and mammals [5], etc. Therefore, many researchers have studied the bifurcation and stability analysis for discrete-time predator–prey system with the Allee effect [3,4,11,18].

Researchers often study the bifurcation phenomenon of a system when its parameters change, including flip bifurcation, transcritical bifurcation, and Neimark–Sacker bifurcation. However, numerous parameters are involved in real models, and when several parameters change at once, the system may undergo more complicated bifurcations. For instance, codimension-2 bifurcation, also known as double crisis, may happen when two system parameters change simultaneously. This phenomenon has been studied in several domains [2, 16, 28]. Research has shown that on a biparameter bifurcation diagram, the system may exhibit Arnold tongue and shrimp-shaped structures, which are not observed in a single-parameter bifurcation diagram [10, 19]. To our knowledge, there is relatively little research on codimension-2 bifurcation in discrete systems. Therefore, in this article, we will study the following discrete predator–prey system with fear effect and Allee effect:

$$\begin{aligned} x_{t+1} &= x_t \exp\left[\frac{r}{1+ky_t}\left(1-\frac{x_t}{K}\right) - by_t\right],\\ y_{t+1} &= y_t \exp\left[\frac{\beta x_t y_t}{h+y_t} - \mu\right], \end{aligned} \tag{1}$$

where x and y represent prey and predator population densities. $K > 0$ is the carrying capacity, $r > 0$ is the intrinsic growth rate of the prey, $b > 0$ is the capture rate, $\beta > 0$ is the conversion coefficient, and $\mu > 0$ is the death rate of the predator. The term $y/(h+y)$ denotes the weak Allee effect function, and $h \geqslant 0$.

The structure of this essay is as follows. Preliminaries are covered in Section 2. In Section 3, we study the necessary conditions of existence for codimension-2 bifurcations connected to resonances of $1:2$, $1:3$, and $1:4$. The theoretical conclusions are illustrated using numerical simulations in Section 4. In Section 5, a succinct discussion is provided.

2 Preliminaries

The equilibrium points for system (1) can be obtained by solving the following equations:

$$\begin{aligned} x &= x \exp\left[\frac{r}{1+ky}\left(1-\frac{x}{K}\right) - by\right],\\ y &= y \exp\left[\frac{\beta xy}{h+y} - \mu\right]. \end{aligned}$$

The following conclusions can be drawn from the calculation:

(I) System (1) always has two equilibrium points $E_0(0,0)$ and $E_K(K,0)$.

(II) System (1) has a unique positive equilibrium point $E^*(x^*, y^*)$, where $x^* = (1/\beta y^*)(\mu h + \mu y^*)$, and y^* is real positive root of the following cubic equation:

$$c_0 y^3 + c_1 y^2 + c_2 y + c_3 = 0,$$

where $c_0 = b\beta k K,\ c_1 = b\beta K,\ c_2 = r\mu - rK\beta,\ c_3 = rh\mu$, if and only if one of the following conditions holds:

(II-1) $q < 0$,

(II-2) $q > 0$ and $q^2/4 + p^3/27 = 0$,

where $(27c_0^2 c_3 - 9c_0 c_1 c_2 + 2c_1^2)/(27c_0^3)$ and $p = (3c_0 c_2 - c_1^2)/(3c_0^2)$.

Jacobian matrix can be evaluated at $E_0(0,0)$ as

$$J(E_0) = \begin{pmatrix} \mathrm{e}^r & -m \\ 0 & \mathrm{e}^{-\mu} \end{pmatrix}.$$

The eigenvalues of the Jacobian are $\lambda_1 = \mathrm{e}^r > 1$ and $\lambda_2 = \mathrm{e}^{-\mu} < 1$ at trivial equilibrium point $E_0(0,0)$. So, we can get the following theorem.

Theorem 1. $E_0(0,0)$ *is always a saddle point, and it is unstable.*

Proof. It is easy to see that the eigenvalues of system (1) at the equilibrium point $E_0(0,0)$ are $\lambda_1 = \mathrm{e}^r$ and $\lambda_2 = \mathrm{e}^{-\mu}$, and $|\lambda_1| > 1$, $|\lambda_2| < 1$. Therefore, $E_0(0,0)$ is a saddle point, and it is unstable. □

Jacobian matrix can be evaluated at $E_K(K,0)$ as

$$J(E_K) = \begin{pmatrix} 1 - r & -bK \\ 0 & \mathrm{e}^{-\mu} \end{pmatrix}.$$

Theorem 2. *The characteristic roots at the boundary equilibrium point* $E_K(K,0)$ *are* $\lambda_1 = 1 - r$ *and* $\lambda_2 = \mathrm{e}^{-\mu}$*, then*

(I) E_K *is a sink point* $\Leftrightarrow 0 < r < 2$;

(II) E_K *is a saddle point* $\Leftrightarrow r > 2$;

(III) E_K *is a nonhyperbolic point* $\Leftrightarrow r = 2$.

Proof. Since the eigenvalues of system (1) at the equilibrium point $E_K(K,0)$ are $\lambda_1 = 1 - r$ and $\lambda_2 = \mathrm{e}^{-\mu}$, therefore, $|\lambda_1| < 1$ if and only if $0 < r < 2$, $|\lambda_2| < 1$ if and only if $\mu > 0$. So E_K is a sink point if and only if $0 < r < 2$. Similarly, (II) and (III) hold. □

$J(x,y)$ evaluated at the positive equilibrium point $E^*(x^*, y^*)$ is

$$J(E^*) = \begin{pmatrix} 1 - \frac{rx^*}{K(1+ky^*)} & -\frac{rkx^*}{(1+ky^*)^2}(1 - \frac{x^*}{K}) - bx^* \\ \frac{\beta y^{*2}}{h+y^*} & 1 + \frac{\beta h x^* y^*}{(h+y^*)^2} \end{pmatrix} := \begin{pmatrix} 1 - A & -B \\ C & 1 + D \end{pmatrix}. \tag{2}$$

Let

$$T(k,h) = 2 + \frac{\beta h x^* y^*}{(h+y^*)^2} - \frac{r x^*}{K(1+ky^*)},$$
$$R(k,h) = \left[1 - \frac{r x^*}{K(1+ky^*)}\right]\left[1 + \frac{\beta h x^* y^*}{(h+y^*)^2}\right] + \frac{\beta y^{*2}}{h+y^*}\left[\frac{rkx^*}{(1+ky^*)^2}\left(1 - \frac{x^*}{K}\right) + bx^*\right].$$

Then the characteristic equation corresponding to matrix (2) is

$$\lambda^2 - T(k,h)\lambda + R(k,h) = 0.$$

Theorem 3. *System* (1) *at the positive equilibrium point* $E^*(x^*, y^*)$ *is local asymptotically stable when all of the following conditions are true*:

(I) $$\frac{rhx^{*2}}{K(1+ky^*)(h+y^*)} < y^*\left[\frac{rkx^*}{(1+ky^*)^2}\left(1 - \frac{x^*}{K}\right) + bx^*\right];$$

(II) $$2\left(2 + \frac{\beta h x^* y^*}{(h+y^*)^2} - \frac{r x^*}{K(1+ky^*)}\right) > \frac{r\beta h x^{*2} y}{K(1+ky^*)(h+y^*)^2} - \frac{\beta y^{*2}}{h+y^*}\left[\frac{rkx^*}{(1+ky^*)^2}\left(1 - \frac{x^*}{K}\right) + bx^*\right];$$

(III) $$\left[1 - \frac{r x^*}{K(1+ky^*)}\right]\left[1 + \frac{\beta h x^* y^*}{(h+y^*)^2}\right] + \frac{\beta y^{*2}}{h+y^*}\left[\frac{rkx^*}{(1+ky^*)^2}\left(1 - \frac{x^*}{K}\right) + bx^*\right] < 1.$$

Proof. According to the Jury condition, the necessary and sufficient condition for the eigenvalue $|\lambda_i| < 1$ $(i = 1, 2)$ of equation $\lambda^2 - T\lambda + R = 0$ is $|T| < R + 1 < 1$. So, we can obtain that unique positive equilibrium point $E^*(x^*, y^*)$ of system (1) is local asymptotically stable if and only if (I), (II), and (III) hold. □

It is easy to get that two eigenvalues of $J(E^*)$ are

$$\lambda_{1,2} = \frac{T \pm \sqrt{T^2 - 4R}}{2}.$$

When system (1) occurs $1:2$ resonance at the equilibrium point $E^*(x^*, y^*)$, the eigenvalue corresponding to (2) is $\lambda_{1,2} = -1$, so that $T = -2$ and $R = 1$. When system (1) occurs $1:3$ resonance at the equilibrium point E^*, the eigenvalue corresponding to (2) is $\lambda_{1,2} = -1/2 \pm (\sqrt{3}/2)\mathrm{i}$, so that $T = -1$ and $R = 1$. At last, if $T = 0$, $R = 1$, we have $\lambda_{1,2} = \pm\mathrm{i}$. In this situation, system (1) exhibits $1:4$ resonance at $E^*(x^*, y^*)$. Therefore, we have the following theorem.

Theorem 4.

(I) *There is a* $1:2$ *strong resonance if* $(r, k, K, b, \beta, h, \mu) \in F_1$, *where*

$$F_1 = \{(r, k, K, b, \beta, h, \mu)\colon T(k_1, h_1) = -2,\ R(k_1, h_1) = 1\}.$$

(II) *There is a* $1:3$ *strong resonance if* $(r,k,K,b,\beta,h,\mu)\in F_2$*, where*

$$F_2=\{(r,k,K,b,\beta,h,\mu)\colon\ T(k_2,h_2)=-1,\ R(k_2,h_2)=1\}.$$

(III) *There is a* $1:4$ *strong resonance if* $(r,k,K,b,\beta,h,\mu)\in F_3$*, where*

$$F_3=\{(r,k,K,b,\beta,h,\mu)\colon\ T(k_3,h_3)=0,\ R(k_3,h_3)=1\}.$$

3 Bifurcation of condimension-two

3.1 Bifurcation with 1 : 2 resonance

Selecting arbitrary parameters $(r,k,K,b,\beta,h,\mu)\in F_1$, system (1) has an unique positive fixed point $E^*(x^*,y^*)$. Let $U=x-x^*$, $V=y-y^*$, then system (1) can be transformed to the following complex form:

$$\begin{bmatrix}U(n+1)\\V(n+1)\end{bmatrix}=\begin{bmatrix}1-A & -B\\ C & 1+D\end{bmatrix}\begin{bmatrix}U(n)\\V(n)\end{bmatrix}+\begin{bmatrix}f(U,V)\\g(U,V)\end{bmatrix}, \tag{3}$$

where

$$f(U,V)=A_{20}U^2+A_{11}UV+A_{02}V^2+A_{30}U^3+A_{21}U^2V+A_{12}UV^2+A_{03}V^3,$$
$$g(U,V)=B_{20}U^2+B_{11}UV+B_{02}V^2+B_{30}U^3+B_{21}U^2V+B_{12}UV^2+B_{03}V^3,$$

and

$$\begin{aligned}
A_{20}&=\frac{r^2kx^*}{2K^2(1+ky^*)^2}-\frac{r(1+k)}{2K(1+ky^*)},\\
A_{11}&=\frac{rk^2x^*}{K(1+ky^*)^2}+\frac{(1-A)B}{x^*},\\
A_{02}&=\frac{rk^2x^*}{(1+ky^*)^3}\left(1-\frac{x^*}{K}\right)-\frac{B(bx^*-B)}{2x^*},\\
A_{30}&=\frac{r^2k}{6K^2(1+ky^*)^2}-\frac{rA_{20}}{3K(1+ky^*)},\\
A_{21}&=\frac{rk(k+1)}{2K(1+ky^*)^2}-\frac{r^2k^2x^*}{K^2(1+ky^*)^2}-\frac{BA_{20}}{x^*},\\
A_{12}&=-\frac{rk^3x^*}{K(1+ky^*)^3}+\frac{rk^2B}{2k(1+ky^*)^2}-\frac{(1-A)rk^2}{(1+ky^*)^3}\left(1-\frac{x^*}{K}\right)\\
&\quad-\frac{rk(1-A)}{2(1+ky^*)^2}\left(1-\frac{x^*}{K}\right),\\
A_{03}&=-\frac{rk^3x^*}{(1+ky^*)^4}\left(1-\frac{x^*}{K}\right)-\frac{r^2k^3x^*}{3(1+ky^*)^5}\left(1-\frac{x^*}{K}\right)^2\\
&\quad-\frac{Brk^2}{3(1+ky^*)^3}\left(1-\frac{x^*}{K}\right)-\frac{BA_{20}}{3x^*},
\end{aligned}$$

$$B_{20} = \frac{\beta^2 y^{*2}}{2(h+y^*)^2}, \qquad B_{11} = \frac{2\beta h y^* - \beta y^{*2}}{(h+y^*)^2} - \frac{\beta^2 h x^* y^{*2}}{(h+y^*)^3},$$
$$B_{02} = \frac{\beta h x^*}{2(h+yr*)} + \frac{\beta h^2 x^* - \beta h x^* y^*}{2(h+y^*)^3} + \frac{\beta^2 h^2 x^{*2} y^*}{2(h+y^*)^4},$$
$$B_{30} = \frac{\beta^3 y^{*3}}{6(h+y^*)^3}, \qquad B_{21} = \frac{3\beta^2 h y^{*2} - \beta^2 y^{*3}}{2(h+y^*)^3} + \frac{\beta^3 h x^* y^{*3}}{2(h+y^*)^4},$$
$$B_{12} = \frac{2\beta h^2 - 2\beta h y^* - \beta y^{*2}}{2(h+y^*)^3} - \frac{2\beta^2 h^2 x^* y^* - \beta^2 h x^* y^*}{2(h+y^*)^4} + \frac{\beta h x^* y^* B_{11}}{2(h+y^*)^2},$$
$$B_{03} = \frac{\beta h x^* y^* - 2\beta h^2 x^*}{3(h+y^*)^4} - \frac{\beta h x^*}{3(h+y^*)^3} + \frac{\beta^2 h^3 x^{*3} - 3\beta^2 h^2 x^{*2} y^*}{6(h+y^*)^5}.$$

Let

$$T = \begin{pmatrix} \frac{bKx^*(1+2ky^*)}{2K(1+ky^*)-rx^*} & \frac{bK^2x^*(1+ky^*)(1+2ky^*)}{[2K(1+ky^*)-rx^*]^2} \\ 1 & 0 \end{pmatrix}. \tag{4}$$

Consider the inverse translation

$$\begin{pmatrix} \widehat{X}(n) \\ \widehat{Y}(n) \end{pmatrix} = T \begin{pmatrix} U(n) \\ V(n) \end{pmatrix},$$

then system (3) takes the form

$$\begin{bmatrix} \widehat{X}(n+1) \\ \widehat{Y}(n+1) \end{bmatrix} = \begin{bmatrix} -1 + A_{10} & 1 + A_{01} \\ B_{10} & -1 + B_{01} \end{bmatrix} \begin{bmatrix} \widehat{X}(n) \\ \widehat{Y}(n) \end{bmatrix} + \begin{bmatrix} \widehat{f}(\widehat{X}(n), \widehat{Y}(n)) \\ \widehat{g}(\widehat{X}(n), \widehat{Y}(n)) \end{bmatrix},$$

where

$$A_{10} = 2 + \frac{h\beta x^* y^*}{(h+y^*)^2} + \frac{b\beta K x^* y^* (1+2ky^*)}{(h+y^*)[2K(1+ky^*) - rx^*]},$$
$$A_{01} = -1 + \frac{b\beta K^2 x^* y^{*2} (1+ky^*)(1+2ky^*)}{(h+y^*)[2K(1+ky^*) - rx^*]^2},$$
$$B_{10} = -\frac{4K(1+ky^*) - 2rx^*}{K(1+ky^*)} - \frac{\beta b K x^* y^{*2} (1+2ky^*)}{K(h+y^*)(1+ky^*)} - \frac{h\beta x^* y^* [2K(1+ky^*) - rx^*]}{K(1+ky^*)(h+y^*)^2},$$
$$B_{01} = 1 + \frac{K(1+ky^*) - rx^*}{K(1+ky^*)} - \frac{bK\beta x^* y^{*2}(1+2ky^*)}{(h+y^*)[2K(1+ky^*) - rx^*]},$$
$$\widehat{f}\big(\widehat{X}(n), \widehat{Y}(n)\big) = \sum_{2 \leqslant i+j \leqslant 3} \hat{A}_{ij} \widehat{X}^i(n) \widehat{Y}^j(n),$$
$$\widehat{g}\big(\widehat{X}(n), \widehat{Y}(n)\big) = \sum_{2 \leqslant i+j \leqslant 3} \hat{B}_{ij} \widehat{X}^i(n) \widehat{Y}^j(n),$$
$$A_1 = \frac{bKx^*(1+2ky^*)}{2K(1+ky^*) - rx^*}, \qquad A_2 = \frac{K(1+ky^*)}{2K(1+ky^*) - rx^*},$$

$$\hat{A}_{20} = A_1^2 B_{20} + A_1 B_{11} + B_{02}, \qquad \hat{A}_{11} = 2A_1^2 A_2 B_{20} + A_1 A_2 B_{11},$$
$$\hat{A}_{02} = A_1^2 A_2^2 B_{20}, \qquad \hat{A}_{30} = A_1^3 B_{30} + A_1^2 B_{21} + A_1 B_{12} + B_{03},$$
$$\hat{A}_{21} = 3A_1^3 A_2 B_{30} + 2A_1^2 A_2 b_{21} + A_1 A_2 B_{12}, \qquad \hat{A}_{12} = 3A_1^3 A_2^2 B_{30} + A_1^2 A_2^2 B_{21},$$
$$\hat{A}_{03} = A_1^3 A_2^3 B_{30}, \qquad \hat{B}_{20} = \frac{1}{A_1 A_2}\left[A_1^2 A_{20} + A_1 A_{11} + A_{02}\right] - \frac{1}{A_2}\hat{A}_{20},$$
$$\hat{B}_{11} = 2A_1 A_{20} + A_{11} - \frac{1}{A_2}\hat{A}_{11}, \qquad \hat{B}_{02} = A_1 A_2 A_{20} - \frac{1}{A_2}\hat{A}_{02},$$
$$\hat{B}_{30} = \frac{1}{A_1 A_2}\left[A_1^3 A_{30} + A_1^2 A_{21} + A_1 A_{12} + A_{03}\right] - \frac{1}{A_2}\hat{A}_{30},$$
$$\hat{B}_{21} = 3A_1^2 A_{30} + 2A_1 A_{21} + A_{12} - \frac{1}{A_2}\hat{A}_{21},$$
$$\hat{B}_{12} = 3A_1^2 A_2 A_{30} + A_1 A_2 A_{21} - \frac{1}{A_2}\hat{A}_{12}, \qquad \hat{B}_{03} = A_1^2 A_2^2 A_{30} - \frac{1}{A_2}\hat{A}_{03}.$$

The following coordinate transformation is performed on system (4):

$$\begin{bmatrix} \widehat{X}(n+1) \\ \widehat{Y}(n+1) \end{bmatrix} = \begin{bmatrix} 1 + A_{01} & 0 \\ -A_{10} & 1 \end{bmatrix} \begin{bmatrix} \bar{X}(n) \\ \bar{Y}(n) \end{bmatrix}.$$

Then system (4) becomes

$$\begin{bmatrix} \bar{X}(n+1) \\ \bar{Y}(n+1) \end{bmatrix} = \begin{bmatrix} -1 & 1 \\ \varrho_1 & -1 + \varrho_2 \end{bmatrix} \begin{bmatrix} \bar{X}(n) \\ \bar{Y}(n) \end{bmatrix} + \begin{bmatrix} P(\bar{X}(n), \bar{Y}(n)) \\ Q(\bar{X}(n), \bar{Y}(n)) \end{bmatrix},$$

where

$$\varrho_1 = B_{10} + A_{01} B_{10} - A_{10} B_{01}, \qquad \varrho_2 = A_{10} + B_{01},$$
$$P\big(\bar{X}(n), \bar{Y}(n)\big) = \sum_{2 \leqslant i+j \leqslant 3} p_{ij} \bar{X}^i(n) \bar{Y}^j(n),$$
$$Q\big(\bar{X}(n), \bar{Y}(n)\big) = \sum_{2 \leqslant i+j \leqslant 3} q_{ij} \bar{X}^i(n) \bar{Y}^j(n),$$

and

$$p_{20} = \frac{1}{1 + A_{01}}\left[(1 + A_{01})^2 \hat{A}_{20} - A_{10}(1 + A_{01})\hat{A}_{11} + A_{10}^2 \hat{A}_{02}\right],$$
$$p_{11} = \frac{1}{A_{01}}\left[(1 + A_{01})\hat{A}_{11} - 2A_{10}\hat{A}_{02}\right], \qquad p_{02} = \frac{\hat{A}_{02}}{1 + A_{01}},$$
$$p_{30} = \frac{1}{1 + A_{01}}\left[(1 + A_{01})^3 \hat{A}_{30} - A_{10}(1 + A_{01})^2 \hat{A}_{21} + A_{10}^2 (1 + A_{01})\hat{A}_{12} - A_{10}^3 \hat{A}_{03}\right],$$
$$p_{21} = \frac{1}{1 + A_{01}}\left[(1 + A_{01})^2 \hat{A}_{21} - 2A_{10}(1 + A_{01})\hat{A}_{12} - 3A_{10}^2 \hat{A}_{03}\right],$$
$$p_{12} = \frac{1}{1 + A_{01}}\left[(1 + A_{01})\hat{A}_{12} - 3A_{10}\hat{A}_{03}\right], \qquad p_{03} = \frac{\hat{A}_{03}}{1 + A_{01}},$$

$$
\begin{aligned}
q_{20} &= A_{10}p_{20} + \hat{b}_{20}(1+A_{01})^2 - A_{10}(1+A_{01})\hat{B}_{11} + A_{10}^2\hat{B}_{02},\\
q_{11} &= A_{10}p_{11} + (1+A_{01})\hat{B}_{11} - 2A_{10}\hat{B}_{02}, \qquad q_{02} = A_{10}p_{02} + \hat{B}_{02},\\
q_{30} &= A_{10}p_{30} + (1+A_{01})^3\hat{B}_{30} - A_{10}(1+A_{01})^2\hat{B}_{21}\\
&\quad + A_{10}^2(1+A_{01})\hat{B}_{12} - A_{10}^3\hat{B}_{03},\\
q_{21} &= A_{10}p_{21} + (1+A_{01})^2\hat{B}_{21} - 2A_{10}(1+A_{01})\hat{B}_{12} - 3A_{10}^2\hat{B}_{03},\\
q_{12} &= A_{10}p_{12} + (1+A_{01})\hat{B}_{12} - 3A_{10}\hat{B}_{03}, \qquad q_{03} = A_{10}p_{03} + \hat{B}_{03}.
\end{aligned}
$$

We introduce the following transformation:

$$
\bar{X} = \kappa_1 + \sum_{2\leqslant i+j\leqslant 3} \varphi_{ij}\kappa_1^i\kappa_2^j, \qquad \bar{Y} = \kappa_2 + \sum_{2\leqslant i+j\leqslant 3} \psi_{ij}\kappa_1^i\kappa_2^j,
$$

where

$$
\begin{aligned}
\varphi_{20} &= \frac{1}{4}q_{20} + \frac{1}{2}p_{20}, \qquad \varphi_{11} = \frac{1}{2}p_{20} + \frac{1}{2}p_{11} + \frac{1}{2}q_{20} + \frac{1}{4}q_{11},\\
\varphi_{02} &= \frac{1}{4}p_{11} + \frac{1}{2}p_{02} + \frac{1}{8}q_{20} + \frac{1}{4}q_{11} + \frac{1}{4}q_{02}, \qquad \varphi_{30} = \frac{1}{9}q_{30},\\
\varphi_{21} &= \frac{1}{2}p_{30} + \frac{1}{2}p_{21} + \frac{5}{12}q_{30} + \frac{1}{4}q_{21},\\
\varphi_{12} &= \frac{1}{6}p_{30} + \frac{1}{2}p_{21} + p_{12} + \frac{17}{36}q_{30} + \frac{3}{4}q_{21} + q_{12},\\
\psi_{20} &= \frac{1}{2}q_{20}, \qquad \psi_{11} = \frac{1}{2}q_{20} + \frac{1}{2}q_{11}, \qquad \psi_{02} = \frac{1}{4}q_{11} + \frac{1}{2}q_{02},\\
\psi_{30} &= \frac{1}{3}q_{30}, \qquad \psi_{21} = \frac{1}{2}q_{30} + \frac{1}{2}q_{21}, \qquad \psi_{12} = \frac{1}{6}q_{30} + \frac{1}{2}q_{21} + q_{12}.
\end{aligned}
$$

Therefore, we obtain the following critical normal form:

$$
\begin{bmatrix}\kappa_1(n+1)\\ \kappa_2(n+1)\end{bmatrix} = \begin{bmatrix}-1 & 1\\ \varrho_1 & -1+\varrho_2\end{bmatrix}\begin{bmatrix}\kappa_1(n)\\ \kappa_2(n)\end{bmatrix} + \begin{bmatrix}0\\ \mathcal{C}_1\kappa_1^3(n) + \mathcal{D}_1\kappa_1^2(n)\kappa_2(n)\end{bmatrix}
$$

with $\mathcal{C}_1$ and $\mathcal{D}_1$ satisfying

$$
\begin{aligned}
\mathcal{C}_1 &= q_{30} + p_{20}q_{20} + \frac{1}{2}q_{20}^2 + \frac{1}{2}q_{20}q_{11},\\
\mathcal{D}_1 &= q_{21} + 3p_{30} + \frac{1}{2}p_{20}q_{11} + \frac{5}{4}q_{20}q_{11} + q_{20}q_{02} + 3p_{20}^2\\
&\quad + \frac{5}{2}p_{20}q_{20} + \frac{5}{2}p_{11}q_{20} + q_{20}^2 + \frac{1}{2}q_{11}^2.
\end{aligned}
$$

Based on the above analysis, we have the following theorem.

Theorem 5. *The nondegeneracy conditions of this bifurcation are as follows*: $\mathcal{C}_1 \neq 0$ *and* $\mathcal{D}_1 + 3\mathcal{C}_1 \neq 0$. *Moreover, if* $\mathcal{C}_1 < 0$, *the fixed point* $E^*(x^*, y^*)$ *is a saddle*; *if* $\mathcal{C}_1 > 0$, *the fixed point* $E^*(x^*, y^*)$ *is elliptic.* $\mathcal{D}_1 + 3\mathcal{C}_1 \neq 0$ *determines the bifurcation scenarios near the* $1:2$ *resonance point.*

3.2 Bifurcation with 1 : 3 resonance

Taking parameters $(r, k, K, b, \beta, h, \mu) \in F_2$, we can get the Jacobian matrix of system (1) at $E^*(x^*, y^*)$ as follows:

$$J(E^*) = \begin{bmatrix} 1-A & -B \\ C & 1+D \end{bmatrix},$$

and it has two eigenvalues $\lambda_{1,2} = -1/2 \pm (\sqrt{3}/2)\mathrm{i}$. So we can calculate the eigenvector $p \in \mathbb{C}^2$ and adjoint eigenvector $q \in \mathbb{C}^2$:

$$p(k_2, h_2) = \begin{bmatrix} B \\ \frac{3}{2} - \frac{\sqrt{3}}{2}\mathrm{i} - A \end{bmatrix}, \qquad q(k_2, h_2) = \begin{bmatrix} \frac{1}{B}(\frac{1}{2} - \frac{\sqrt{3}}{2}\mathrm{i} + \frac{\sqrt{3}}{3}A\mathrm{i}) \\ \frac{\sqrt{3}}{3}\mathrm{i} \end{bmatrix},$$

where k_2 and h_2 satisfy $T(k_2, h_2) = -1$ and $R(k_2, h_2) = 1$.

Any vector $W(n) = (x(n), y(n))^{\mathrm{T}} \in \mathbb{R}^2$ can be represented in the form $W = \varpi p + \bar{\varpi}\bar{p}$. Consequently, system (3) can be transformed into

$$\varpi \to -\frac{1}{2} \pm \frac{\sqrt{3}}{2}\mathrm{i}\varpi + \sum_{2 \leqslant i+j \leqslant 3} \frac{\chi_{ij}}{i!j!}\varpi^i \bar{\varpi}^j, \tag{5}$$

where

$$\begin{aligned}
\chi_{20} &= -\frac{2\sqrt{3}\mathrm{i}}{3B}\left(\frac{3}{2} - A - \frac{\sqrt{3}}{2}\mathrm{i}\right)\left[A_{20}p_1^2 + A_{11}p_1p_2 + A_{02}p_2^2\right] \\
&\quad + \frac{2\sqrt{3}}{3}\mathrm{i}\left[B_{20}p_1^2 + B_{11}p_1p_2 + B_{02}p_2^2\right], \\
\chi_{11} &= -\frac{\sqrt{3}\mathrm{i}}{3B}\left(\frac{3}{2} - A - \frac{\sqrt{3}}{2}\mathrm{i}\right)\left[2A_{20}p_1^2 + (p_1\bar{p}_2 + p_1p_2)A_{11} + 2p_2\bar{p}_2A_{02}\right] \\
&\quad + \frac{\sqrt{3}}{3}\mathrm{i}\left[2B_{20}p_1^2 + (p_1\bar{p}_2 + p_1p_2)B_{11} + 2p_2\bar{p}_2B_{02}\right], \\
\chi_{02} &= -\frac{2\sqrt{3}\mathrm{i}}{3B}\left(\frac{3}{2} - A - \frac{\sqrt{3}}{2}\mathrm{i}\right)\left[A_{20}p_1^2 + A_{11}p_1\bar{p}_2 + A_{02}\bar{p}_2^2\right] \\
&\quad + \frac{2\sqrt{3}}{3}\mathrm{i}\left[B_{20}p_1^2 + B_{11}p_1\bar{p}_2 + B_{02}\bar{p}_2^2\right], \\
\chi_{30} &= -\frac{6\sqrt{3}\mathrm{i}}{3B}\left(\frac{3}{2} - A - \frac{\sqrt{3}}{2}\mathrm{i}\right)\left[A_{30}p_1^3 + p_1^2p_2A_{21} + p_1p_2^2A_{12} + p_2^3A_{03}\right] \\
&\quad + 2\sqrt{3}\mathrm{i}\left[B_{30}p_1^3 + p_2^2p_2B_{21} + p_1p_2^2B_{12} + p_2^3B_{03}\right], \\
\chi_{21} &= -\frac{2\sqrt{3}\mathrm{i}}{3B}\left(\frac{3}{2} - A - \frac{\sqrt{3}}{2}\mathrm{i}\right) \\
&\quad \times \left[3p_1^3A_{30} + \left(p_1^2\bar{p}_2 + 2p_1^2p_2\right)A_{21} + (2p_1p_2\bar{p}_2 + p_1p_2^2)A_{12} + 3p_2^2\bar{p}_2A_{03}\right] \\
&\quad + \frac{2\sqrt{3}}{3}\mathrm{i}\left[3p_1^3B_{30} + \left(p_1^2\bar{p}_2 + 2p_1^2p_2\right)B_{21} + \left(2p_1p_2\bar{p}_2 + p_1p_2^2\right)B_{12} + 3p_2^2\bar{p}_2B_{03}\right],
\end{aligned}$$

$$\chi_{12} = -\frac{2\sqrt{3}\mathrm{i}}{3B}\left(\frac{3}{2} - A - \frac{\sqrt{3}}{2}\mathrm{i}\right) \times \left[3p_1^3 A_{30} + 3p_1^2 p_2 A_{21} + (p_1\bar{p}_2^2 + 2p_1p_2\bar{p}_2)A_{12} + 3p_2\bar{p}_2^2 A_{03}\right] + \frac{2\sqrt{3}}{3}\mathrm{i}\left[3p_1^3 B_{30} + 3p_1^2 p_2 B_{21} + (p_1\bar{p}_2^2 + 2p_1p_2\bar{p}_2)B_{12} + 3p_2\bar{p}_2^2 B_{03}\right],$$

$$\chi_{03} = -\frac{6\sqrt{3}\mathrm{i}}{3B}\left(\frac{3}{2} - A - \frac{\sqrt{3}}{2}\mathrm{i}\right)\left[A_{30}p_1^3 + p_1^2p_2A_{21} + p_1\bar{p}_2^2A_{12} + \bar{p}_2^3A_{03}\right] + 2\sqrt{3}\mathrm{i}\left[B_{30}p_1^3 + p_1^2p_2B_{21} + p_1\bar{p}_2^2B_{12} + \bar{p}_2^3B_{03}\right].$$

Next, we will introduce the following transformation to eliminate some quadratic terms in (5). Let

$$\varpi(n) = w(n) + \frac{1}{2}\nu_{20}w^2(n) + \nu_{11}w(n)\bar{w}(n) + \frac{1}{2}\bar{w}^2(n). \tag{6}$$

The inverse transformation of (6) is

$$w(n) = \varpi(n) - \frac{\nu_{20}}{2}\varpi^2(n) - \nu_{11}\varpi(n)\bar{\varpi}(n) - \frac{\nu_{02}}{2}\bar{\varpi}^2(n) + \frac{1}{2}\left(\nu_{20}^2 + \nu_{11}\bar{\nu}_{02}\right)\varpi^3(n) + \left(|\nu_{11}|^2 + \frac{3}{2}\nu_{11}\nu_{20} + \frac{1}{2}|\nu_{02}|^2\right)\varpi^2(n)\bar{\varpi}(n) + \frac{1}{2}(\nu_{11}\nu_{02} + \nu_{02}\bar{\nu}_{20})\bar{\varpi}^3(n) + \left(\nu_{20}\bar{\nu}_{11} + \nu_{11}^2 + \frac{1}{2}\nu_{11}\bar{\nu}_{20} + \frac{1}{2}\nu_{20}\nu_{02}\right)\varpi(n)\bar{\varpi}^2(n) + O\left(\left|\varpi(n)\right|^4\right).$$

Bringing (6) into (5), we can get

$$w(n+1) = \lambda_1\varpi + \sum_{2\leqslant i+j\leqslant 3}\frac{\sigma_{ij}}{i!j!}w^i\bar{w}^j + O\left(\left|w(n)\right|^4\right), \tag{7}$$

where

$$\sigma_{20} = \lambda_1\nu_{20} + \chi_{20} - \lambda_1^2\nu_{20}, \qquad \sigma_{11} = \lambda_1\nu_{11} + \chi_{11} - |\lambda_1|^2\nu_{11},$$

$$\sigma_{02} = \lambda_1\nu_{02} + \chi_{02} - \overline{\lambda}_1^2\nu_{02},$$

$$\sigma_{30} = 3(1-\lambda_1)\chi_{20}\nu_{20} + 3\chi_{11}\bar{\nu}_{02} + \chi_{30} + 3\lambda_1^2(\lambda_1 - 1)\nu_{20}^2 + 3\left(\lambda_1^3 - |\lambda_1|^2\right)\nu_{11}\bar{\nu}_{02} - 3\lambda_1\bar{\chi}_{02}\nu_{11},$$

$$\sigma_{21} = 2\chi_{11}\bar{\nu}_{11} + \chi_{11}\nu_{20} + 2\chi_{20}\nu_{11} + \chi_{02}\bar{\nu}_{02} + \chi_{21} + 2\lambda_1^2(\overline{\lambda}_1 - 1)\nu_{20}\nu_{11} - 2\lambda_1\chi_{11}\nu_{20} - \overline{\lambda}_1\bar{\chi}_{02}\nu_{02} + 2|\lambda_1|^2(\lambda_1 - 1)|\nu_{11}|^2 + |\lambda_1|^2(\lambda_1 - 1)\nu_{11}\nu_{20} - 2\lambda_1\nu_{11}\bar{\chi}_{11} - \overline{\lambda}_1\chi_{20}\nu_{11} + \overline{\lambda}_1\left(\lambda_1^2 - \overline{\lambda}_1\right)|\nu_{02}|^2,$$

$$\sigma_{12} = 2\chi_{11}\nu_{11} + \chi_{11}\bar{\nu}_{20} + 2\chi_{02}\bar{\nu}_{11} + \chi_{20}\nu_{02} + \chi_{12} + \lambda_1\left(\overline{\lambda}_1^2 - \lambda_1\right)\nu_{20}\nu_{02} - \lambda_1\chi_{02}\nu_{20} + 2|\lambda_1|^2(\overline{\lambda}_1 - 1)\nu_{11}^2 + |\lambda_1|^2(\overline{\lambda}_1 - 1)\nu_{11}\bar{\nu}_{20} - \lambda_1\nu_{11}\bar{\chi}_{20} - 2\overline{\lambda}_1\chi_{11}\nu_{11} + 2\overline{\lambda}_1(\lambda_1 - 1)\nu_{02}\bar{\nu}_{11} - 2\overline{\lambda}_1\bar{\chi}_{11}\nu_{02},$$

$$\sigma_{03} = 3\chi_{11}\nu_{02} + 3\chi_{02}\bar{\nu}_{20} + \chi_{03} + 3\left(\overline{\lambda}_1^3 - |\lambda_1|^2\right)\nu_{11}\nu_{02} - 3\overline{\lambda}_1\chi_{02}\nu_{11} + 3\overline{\lambda}_1(\overline{\lambda}_1 - 1)\nu_{02}\bar{\nu}_{20} - 2\overline{\lambda}_1\bar{\chi}_{20}\nu_{02}.$$

Obviously, we have

$$\lambda_1^2(k_2,h_2) - \lambda_1(k_2,h_2) \neq 0, \qquad \left|\lambda_1(k_2,h_2)\right|^2 - \lambda_1(k_2,h_2) \neq 0,$$
$$\overline{\lambda}_1^2(k_2,h_2) - \lambda_1(k_2,h_2) = 0.$$

Therefore, we can take

$$\nu_{20} = \frac{\chi_{20}}{\lambda_1^2 - \lambda_1}, \qquad \nu_{11} = \frac{\chi_{11}}{|\lambda_1|^2 - \lambda_1}, \qquad \nu_{02} = 0.$$

The next step is to annihilate cubic terms, we take

$$w(n) = \kappa(n) + \frac{1}{6}\nu_{30}\kappa^3(n) + \frac{1}{2}\nu_{21}\kappa^2(n)\overline{\kappa}(n) + \frac{1}{2}\nu_{12}\kappa(n)\overline{\kappa}^2(n) + \frac{1}{6}\nu_{03}\overline{\kappa}^3(n). \quad (8)$$

Using (8) and its inverse transformation, (7) becomes

$$\kappa(n+1) = \lambda_1\kappa(n) + \frac{1}{2}\chi_{02}\overline{\kappa}^2(n) + \sum_{i+j=3}\frac{\vartheta_{ij}}{i!j!}\kappa^i(n)\overline{\kappa}^j(n) + O\left(\left|\kappa(n)\right|^4\right),$$

where

$$\vartheta_{30} = \left(\lambda_1 - \lambda_1^3\right)\nu_{30} + \sigma_{30}, \qquad \vartheta_{21} = \left(\lambda_1 - \lambda_1^2\overline{\lambda}_1\right)\nu_{21} + \sigma_{21},$$
$$\vartheta_{12} = \left(\lambda_1 - \lambda_1\overline{\lambda}_1^2\right)\nu_{12} + \sigma_{12}, \qquad \vartheta_{03} = \left(\lambda_1 - \overline{\lambda}_1^3\right)\nu_{03} + \sigma_{03}.$$

Thus, we can take

$$\nu_{30} = \frac{\sigma_{30}}{\lambda_1^3 - \lambda_1}, \qquad \nu_{12} = \frac{\sigma_{12}}{\overline{\lambda}_1|\lambda_1|^2 - \lambda_1}, \qquad \nu_{03} = \frac{\sigma_{03}}{\overline{\lambda}_1^3\lambda_1}, \qquad \nu_{21} = 0.$$

Then the normal form at $1:3$ resonance point is derived as

$$\kappa(n+1) = \lambda_1\kappa(n) + \frac{1}{2}\chi_{02}\overline{\kappa}^2(n) + \frac{1}{2}\sigma_{21}\kappa(n)^2\overline{\kappa}(n) + O\left(\left|\kappa(n)\right|^4\right).$$

Let

$$\mathcal{C}_2 = -\frac{3}{4}(1+\sqrt{3}\mathrm{i})\chi_{02}, \qquad \mathcal{D}_2 = -\frac{3}{4}|\chi_{02}|^2 - \frac{3}{4}(1+\sqrt{3}\mathrm{i})\sigma_{21}.$$

Based on the above analysis, we have the following theorem.

Theorem 6. *Let $k = k_2$ and $h = h_2$. If $\mathcal{C}_2 \neq 0$ and $\operatorname{Re}\mathcal{D}_2 \neq 0$, then system* (1) *undergoes a $1:3$ resonance bifurcation at equilibrium $E^*(x^*, y^*)$. Moreover, $\operatorname{Re}\mathcal{D}_2 \neq 0$ determines the stability of the bifurcation invariant closed curve.*

3.3 Bifurcation with 1 : 4 resonance

The Jacobian matrix of system (1) at $E^*(x^*, y^*)$ is

$$J(E^*) = \begin{pmatrix} 1-A & -B \\ C & 1+D \end{pmatrix}, \quad (9)$$

and when the parameters $(r, k, K, b, \beta, h, \mu) \in F_3$, (9) has two eigenvalues $\lambda_{1,2} = \pm\mathrm{i}$. It is easy to derive the corresponding eigenvalues $p \in \mathbb{C}^2$ and the adjoint eigenvector

$q \in \mathbb{C}^2$ as follows:

$$p(k_3, h_3) = \begin{bmatrix} 1 + D - \mathrm{i} \\ -C \end{bmatrix}, \qquad q(k_3, h_3) = \begin{bmatrix} \frac{\mathrm{i}}{2} \\ \frac{(\mathrm{i}+1-D)\mathrm{i}}{2C} \end{bmatrix},$$

where k_3 and h_3 satisfy $T(k_3, h_3) = 0$ and $R(k_3, h_3) = 1$.

Any vector $W(n) = (x(n), y(n))^{\mathrm{T}} \in \mathbb{R}^2$ can be represented in the form $W = \varpi p + \bar{\varpi}\bar{p}$. Consequently, system (3) can be transformed into

$$\varpi \to \mathrm{i}\varpi + \sum_{2 \leqslant i+j \leqslant 3} \frac{\chi_{ij}}{i!j!} \varpi^i \bar{z}^j, \tag{10}$$

where

$$\begin{aligned}
\chi_{20} &= \mathrm{i}\big[A_{20}p_1^2 + A_{11}p_1p_2 + A_{02}p_2^2\big] + \frac{(\mathrm{i}+1-D)\mathrm{i}}{C}\big[B_{20}p_1^2 + B_{11}p_1p_2 + B_{02}p_2^2\big], \\
\chi_{11} &= \frac{\mathrm{i}}{2}\big[2A_{20}p_1\bar{p}_1 + (p_1p_2 + \bar{p}_1p_2)A_{11} + 2p_2^2A_{02}\big] \\
&\quad + \frac{(\mathrm{i}+1-D)\mathrm{i}}{2C}\big[2B_{20}p_1\bar{p}_1 + (p_1p_2 + \bar{p}_1p_2)B_{11} + 2p_2^2B_{02}\big], \\
\chi_{02} &= \mathrm{i}\big[A_{20}\bar{p}_1^2 + A_{11}\bar{p}_1p_2 + A_{02}p_2^2\big] + \frac{(\mathrm{i}+1-D)\mathrm{i}}{C}\big[B_{20}\bar{p}_1^2 + B_{11}\bar{p}_1p_2 + B_{02}p_2^2\big], \\
\chi_{30} &= 3\mathrm{i}\big[A_{30}p_1^3 + p_1^2p_2A_{21} + p_1p_2^2A_{12} + p_2^3A_{03}\big] \\
&\quad + \frac{3(\mathrm{i}+1-D)\mathrm{i}}{C}\big[B_{30}p_1^3 + p_2^2p_2B_{21} + p_1p_2^2B_{12} + p_2^3B_{03}\big], \\
\chi_{21} &= \mathrm{i}\big[3p_1\bar{p}_1^2A_{30} + \big(p_1^2p_2 + 2p_1\bar{p}_1p_2\big)A_{21} + \big(2p_1p_2^2 + \bar{p}_1p_2^2\big)A_{12} + 3p_2^3A_{03}\big] \\
&\quad + \frac{(\mathrm{i}+1-D)\mathrm{i}}{C}\big[3p_1\bar{p}_1^2B_{30} + \big(p_1^2p_2 + 2p_1\bar{p}_1p_2\big)B_{21} \\
&\quad + \big(2p_1p_2^2 + \bar{p}_1p_2^2\big)B_{12} + 3p_2^3B_{03}\big], \\
\chi_{12} &= \mathrm{i}\big[3p_1\bar{p}_1^2A_{30} + \big(\bar{p}_1^2p_2 + 2p_1\bar{p}_1p_2\big)A_{21} + \big(2\bar{p}_1p_2^2 + p_1p_2^2\big)A_{12} + 3p_2^3A_{03}\big] \\
&\quad + \frac{(\mathrm{i}+1-D)\mathrm{i}}{C}\big[3p_1\bar{p}_1^2B_{30} + \big(\bar{p}_1^2p_2 + 2p_1\bar{p}_1p_2\big)B_{21} \\
&\quad + \big(2\bar{p}_1p_2^2 + p_1p_2^2\big)B_{12} + 3p_2^3B_{03}\big], \\
\chi_{03} &= 3\mathrm{i}\big[A_{30}\bar{p}_1^3 + \bar{p}_1^2p_2A_{21} + \bar{p}_1p_2^2A_{12} + p_2^3A_{03}\big] \\
&\quad + \frac{3(\mathrm{i}+1-D)\mathrm{i}}{2C}\big[B_{30}\bar{p}_1^3 + \bar{p}_1^2p_2B_{21} + \bar{p}_1p_2^2B_{12} + p_2^3B_{03}\big].
\end{aligned}$$

Similar as in Section 3.3, by (6) we can transform (10) into the following form:

$$w(n+1) = \lambda_1\varpi + \sum_{2 \leqslant i+j \leqslant 3} \frac{\sigma_{ij}}{i!j!} w^i \bar{w}^j + O\big(\big|w(n)\big|^4\big). \tag{11}$$

Obviously, we have

$$\lambda_1^2(k_2, h_2) - \lambda_1(k_2, h_2) \neq 0, \qquad \big|\lambda_1(k_2, h_2)\big|^2 - \lambda_1(k_2, h_2) \neq 0,$$
$$\overline{\lambda}_1^2(k_2, h_2) - \lambda_1(k_2, h_2) = 0.$$

Therefore, we can take

$$\nu_{20} = \frac{\mathrm{i}-1}{2}\chi_{20}, \qquad \nu_{11} = \frac{\mathrm{i}+1}{2}\chi_{11}, \qquad \nu_{02} = \frac{1+\mathrm{i}}{2}\chi_{02}.$$

Using (11) and its inverse transformation, (10) becomes

$$\kappa(n+1) = \lambda_1\kappa(n) + \sum_{2\leqslant i+j\leqslant 3} \frac{\vartheta_{ij}}{i!j!}\kappa^i(n)\overline{\kappa}^j(n) + O\big(\big|\kappa(n)\big|^4\big),$$

where

$$\vartheta_{30} = 2\mathrm{i}\nu_{30} + \sigma_{30}, \qquad \vartheta_{21} = \sigma_{21},$$
$$\vartheta_{12} = 2\mathrm{i}\nu_{12} + \sigma_{12}, \qquad \vartheta_{03} = \sigma_{03}.$$

Thus, we can take

$$\nu_{30} = \frac{\mathrm{i}}{2}\sigma_{30}, \qquad \nu_{12} = \frac{\mathrm{i}}{2}\sigma_{12}, \qquad \nu_{03} = 0.$$

Then the normal form at $1:4$ resonance point is derived as

$$\kappa(n+1) = \lambda_1\kappa(n) + \mathcal{C}\kappa(n)\big|\kappa(n)\big|^2 + \mathcal{D}\overline{\kappa}^3(n) + O\big(\big|\kappa(n)\big|^4\big),$$

where

$$\mathcal{C} = \frac{1+3\mathrm{i}}{4}\chi_{11}\chi_{20} + \frac{1-\mathrm{i}}{2}|\chi_{11}|^2 - \frac{1+\mathrm{i}}{4}|\chi_{02}|^2 + \frac{1}{2}\chi_{21},$$
$$\mathcal{D} = \frac{\mathrm{i}-1}{4}\chi_{02}\chi_{11} - \frac{1+\mathrm{i}}{4}\chi_{11}\chi_{20} + \frac{1}{6}\chi_{03}.$$

Let

$$\mathcal{C}_3 = -4\mathrm{i}\mathcal{C}, \qquad \mathcal{D}_3 = -4\mathrm{i}\mathcal{D}.$$

If $\mathcal{D}_3 \neq 0$, we denote $M = \mathcal{C}_3/|\mathcal{D}_3|$.

Based on the above analysis, we have the following theorem.

Theorem 7. *Let $k = k_3$ and $h = h_3$. The bifurcation scenario near the $1:4$ resonance point is determined by $M = \mathcal{C}_3/|\mathcal{D}_3|$. If $\operatorname{Re} M \neq 0$ and $\operatorname{Im} M \neq 0$, then system* (1) *undergoes a $1:4$ resonance bifurcation.*

4 Numerical simulations

In this section, we will analyze the effects of fear effect and Allee effect on population dynamics through numerical simulation. Throughout the numerical simulation, we have kept fixed the values of seven parameters involved in the system, and those parameters' values are

$$r = 2.9, \quad K = 8, \quad b = 0.8, \quad \beta = 0.4, \quad \mu = 0.2.$$

Also, we choose $(1, 1)$ as our initial condition unless stated otherwise.

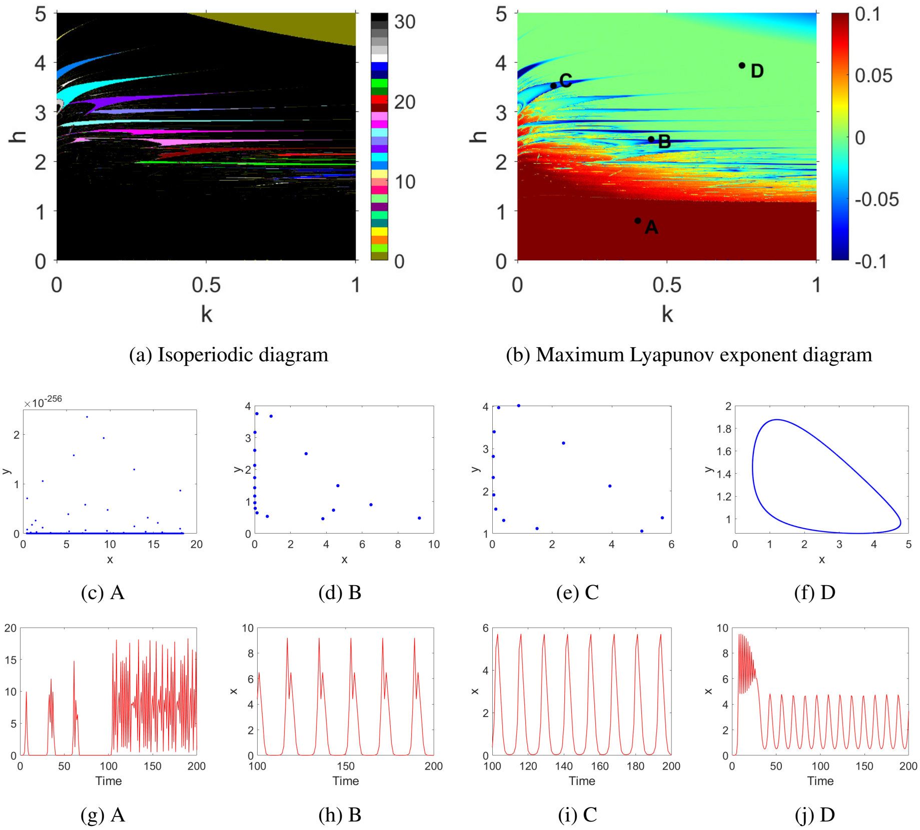

(a) Isoperiodic diagram (b) Maximum Lyapunov exponent diagram

(c) A (d) B (e) C (f) D

(g) A (h) B (i) C (j) D

Figure 1. (a) The isoperiodic diagram. (b) The maximum Lyapunov exponent diagram. (c), (d) The phase-portraits (x_n, y_n) and time series (x_n, n) represent chaos attractor for $(k, h) = (0.414, 0.718)$. (d), (h) Periodic-18 attractor for $(k, h) = (0.47, 2.4)$. (e), (i) Periodic-13 attractor for $(k, h) = (0.11, 3.53)$. (f), (j) Quasiperiodic attractor for $(k, h) = (0.75, 3.9)$.

Figures 1(a), 1(b) show the isoperiodic graph and the maximum Lyapunov exponent (MLE) graph of system (1) in a biparameter space, where different periods in Fig. 1(a) correspond to different colors, and periods greater than 30 are uniformly represented in black. In Fig. 1(b), yellow to red regions are used to describe chaotic regions, and green to blue regions are used to describe periodic attractors (i.e., the maximum Lyapunov exponent is less than 0). From Fig. 1 it is observed that the parameter plane contains a number of V-shaped periodic islands (Arnold tongues). From Fig. 1(b) it is known that the color at point A is red, i.e., MLE > 0. Therefore, the system is in a chaotic state, and the phase diagram and time series diagram of the system at point A are shown in Fig. 1(c). The color of Arnold's tongue at points B and C is blue, and thus MLE < 0. Corresponding to Fig. 1(a), it is known that the system will produce the solution of period-18 at point B and the solution of period-13 at point C. The corresponding phase diagrams and time series diagrams are shown in Figs. 1(d), 1(h) and Figs. 1(e), 1(i).

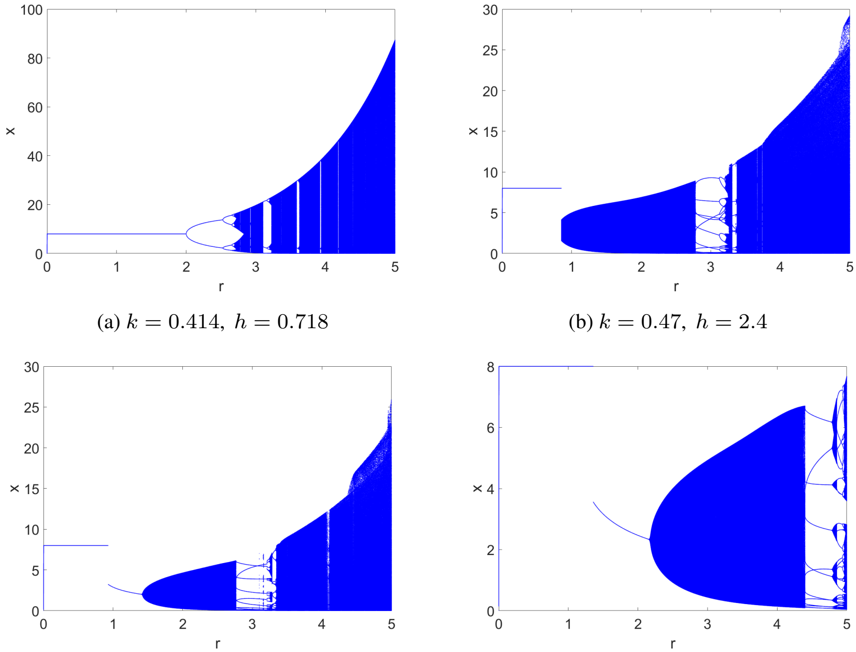

(a) $k = 0.414,\ h = 0.718$ (b) $k = 0.47,\ h = 2.4$

(c) $k = 0.11,\ h = 3.53$ (d) $k = 0.75,\ h = 3.9$

Figure 2. The bifurcation diagram of system (1) when k and h take different values.

At point D, where the MLE value of the system is near 0, the system generates limit loops and thus periodic solutions; see Figs. 1(f), 1(j).

From Fig. 2 it can be observed that when the parameters of the fear effect and the Allee effect change simultaneously, the model transitions between flip bifurcations and Neimark–Sacker bifurcations. This transition implies that the relationship between predators and prey becomes more complex. For instance, the originally stable predator–prey cycles may be disrupted, leading to more variable interaction patterns. This could affect the survival strategies of both species such as the predator's foraging efficiency or the prey's defensive mechanisms.

Figure 3 is a partially enlarged view of Fig. 1. This gives a closer look at the Arnold tongues and their formation. From Fig. 3(a) we see that the ordering of the appeared tongues is based on the periods of the attractors, and the periods of the larger noticeable tongues are increasing (by one) in order from left to right. From this figure it is also observed that there are many smaller tongues in between each pair of larger tongues, and the tongues appearing in the middle of two adjacent larger tongues show other period-adding phenomena, where the period of the largest tongue in the middle of two tongues is equal to the sum of the periods of its adjacent larger tongues. By observing Fig. 3(a) then one can see that the period of the largest tongue between period-13 and period-14 tongues is 27. Similarly, 27 is the period of the largest tongue located between the period-13 and

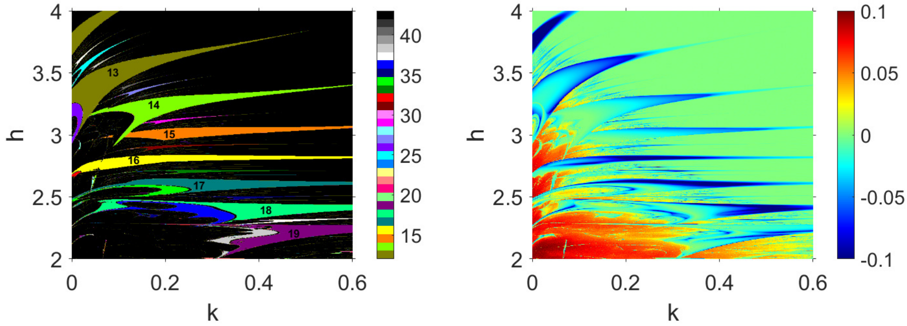

(a) (b)

Figure 3. (a) The isoperiodic diagram. (b) The maximum Lyapunov exponent diagram.

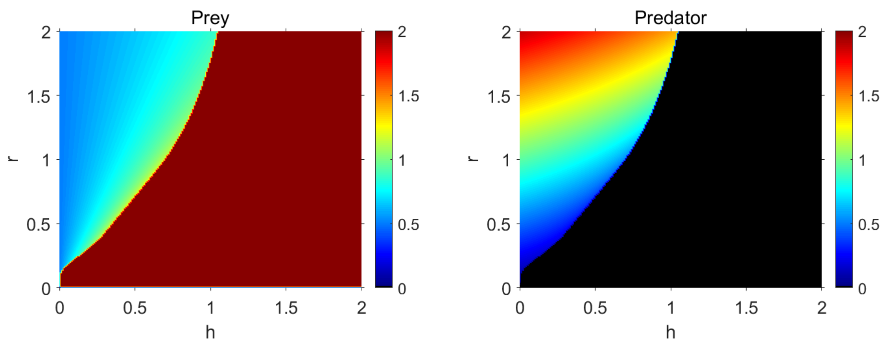

Figure 4. Variation of the densities of prey and predator populations in h, r-biparameter space. Other parameter values are $K = 2$, $b = 0.8$, $\beta = 0.2$, $\mu = 0.1$, and $k = 0$.

period-14 tongues. The period of the largest tongue between period-14 and period-15 tongues is 29, and so on.

The Arnold tongue is a geometric structure that appears in bifurcation diagrams, indicating the region where specific periodic behaviors exist. The Arnold tongue can delineate the parameter range conducive to the coexistence of predators and prey. An appropriate fear effect and Allee effect intensity can enable the two species to interact within a stable period, preventing one from overgrowing or going extinct. This periodic interaction may provide a space for survival for both parties, promoting the maintenance of biodiversity.

In Fig. 4, we explore the effects of prey growth rate r and Allee effect h on prey and predator population density. Here we find that when h is small and the prey growth rate r increases, the population density of predator and prey will increase. When the Allee effect parameter h is large, the predator density approaches 0, and the prey population density approaches K (environmental capacity). When the prey growth rate r remains unchanged, the increase of the Allee effect h will lead to a gradual decrease in the predator population density and region 0, while the prey population density gradually increases and region K. Similarly, we consider the effect of the fear effect k and the predator natural mortality μ

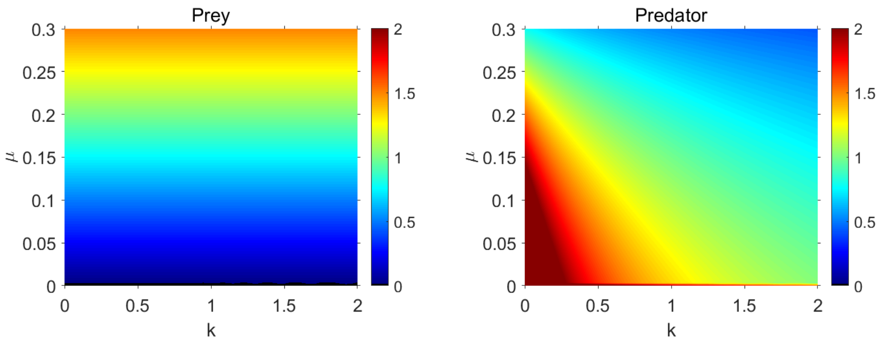

Figure 5. Variation of the densities of prey and predator populations in k, μ-biparameter space. Other parameter values are $K = 2$, $b = 0.8$, $\beta = 0.2$, $r = 2.5$, and $h = 0$.

on the prey and predator population density in Fig. 5. Through observation, it is found that when the fear effect k remains unchanged, the increase of μ will lead to the decrease of predator population density and the increase of prey population density. When the predator's natural mortality μ remains unchanged, the increase of the fear effect k will lead to a decrease in the predator population density, but has no significant effect on the prey population density.

5 Conclusion

In this paper, we give a detailed analysis for the codimension-2 bifurcation of a discrete predator–prey model with fear effect and Allee effect. The theoretical analyses demonstrate that system (1) undergoes $1:2$, $1:3$, and $1:4$ strong resonances by the bifurcation theory. The numerical results show that system (1) will produce Arnold tongue structures in the two-parameter space, which marks the generation of periodic structure. This is a phenomenon not found in codimension-1 bifurcation, and when the parameters of the fear effect and Allee effect take different values, system (1) will produce different bifurcation phenomena. The conclusion obtained in this paper will be useful in the study of applications with predator–prey systems undergoing the codimension-2 bifurcations unfolded by system (1). It is still a challenging problem to explore a multiple parameters bifurcation in the system. We expect to get more analysis results on this issue in the future.

Author contributions. The authors (C.L. and X.H.) have contributed as follows: conceptualization, methodology, investigation, supervision, writing – review and editing, visualization, X.H.; conceptualization, methodology, software, formal analysis, investigation, writing – original draft, C.L. All authors have read and approved the published version of the manuscript.

Conflicts of interest. The authors declare no conflicts of interest.

References

1. Z. AlSharawi, N. Pal, J. Chattopadhyay, The role of vigilance on a discrete-time predator-prey model, *Discrete Contin. Dyn. Syst., Ser. B*, **27**:6723–6744, 2022, `https://doi.org/10.3934/dcdsb.2022017`.
2. L. Bo, Z.M. He, 1:2 and 1:4 resonances in a two-dimensional discrete Hindmarsh–Rose model, *Nonlinear Dyn.*, **79**:705–720, 2015, `https://doi.org/10.1007/s11071-014-1696-3`.
3. P. Chakraborty, S. Sarkar, U. Ghosh, Stability and bifurcation analysis of a discrete prey–predator model with sigmoid functional response and Allee effect, *Rend. Circ. Mat. Palermo (2)*, **70**:253–273, 2021, `https://doi.org/10.1007/s12215-020-00495-5`.
4. L.F. Cheng, H.J. Cao, Bifurcation analysis of a discrete-time ratio-dependent predator–prey model with Allee effect, *Commun. Nonlinear Sci. Numer. Simul.*, **38**:288–302, 2016, `https://doi.org/10.1016/j.cnsns.2016.02.038`.
5. F. Courchamp, B.T. Grenfell, T. Clutton-Brock, Impact of natural enemies on obligately cooperative breeders, *Oikos*, **91**(2):311–322, 2000, `https://doi.org/10.1034/j.1600-0706.2000.910212.x`.
6. S. Debgopal, S. Guruprasad, Oscillatory and transient dynamics of a slow–fast predator–prey system with fear and its carry-over effect, *Nonlinear Anal., Real World Appl.*, **73**:103888, 2023, `https://doi.org/10.1016/j.nonrwa.2023.103888`.
7. Q. Din, Complexity and chaos control in a discrete-time prey-predator model, *Commun. Nonlinear Sci. Numer. Simul.*, **49**:113–134, 2017, `https://doi.org/10.1016/j.cnsns.2017.01.025`.
8. M.J. Groom, Allee effects limit population viability of an annual plant, *Am. Nat.*, **151**(6):487–496, 1998, `https://doi.org/10.1086/286135`.
9. X.L. Han, C.Y. Lei, Bifurcation and turing instability analysis for a space- and time-discrete predator–prey system with Smith growth function, *Chaos Solitons Fractals*, **166**:112910, 2023, `https://doi.org/10.1016/j.chaos.2022.112910`.
10. M. Hossain, S. Garai, S. Jafari, N. Pal, Bifurcation, chaos, multistability, and organized structures in a predator-prey model with vigilance, *Chaos*, **32**(6):063139, 2022.
11. S. Içık, A study of stability and bifurcation analysis in discrete-time predator–prey system involving the Allee effect, *Int. J. Biomath.*, **12**:1950011, 2018, `https://doi.org/10.1142/S1793524519500116`.
12. R.P. Kaur, A. Sharma, A.K. Sharma, Impact of fear effect on plankton-fish system dynamics incorporating zooplankton refuge, *Chaos Solitons Fractals*, **143**:110563, 2021, `https://doi.org/10.1016/j.chaos.2020.110563`.
13. C. Lei, X. Han, W. Wang, Bifurcation analysis and chaos control of a discrete-time prey-predator model with fear factor, *Math. Biosci. Eng.*, **19**(7):6659–6679, 2022, `https://doi.org/10.3934/mbe.2022313`.
14. C.Y. Lei, X.L. Han, W.M. Wang, Bifurcation and stability analysis of a discrete predator–prey model with alternative prey, *Qual. Theory Dyn. Syst.*, **23**:233, 2024, `https://doi.org/10.1007/s12346-024-01092-y`.
15. H.M. Li, Y. Tian, Dynamic behavior analysis of a feedback control predator-prey model with exponential fear effect and Hassell-Varley functional response, *J. Franklin Inst.*, **360**(4):3479–3498, 2023, `https://doi.org/10.1016/j.jfranklin.2022.11.030`.

16. G.W. Lou, Y.L. Zhang, J.H. Xie, Bifurcation sequences of vibroimpact systems near a 1:2 strong resonance point, *Nonlin. Anal., Real World Appl.*, **10**(1):1–15, 2009, https://doi.org/10.1016/j.nonrwa.2007.08.027.
17. R.M. May, Simple mathematical models with very complicated dynamics, *Nature*, **261**:459–467, 1976, https://doi.org/10.1038/261459a0.
18. S. Pal, S.K. Sasmal, N. Pal, Chaos control in a discrete-time predator–prey model with weak Allee effect, *Int. J. Biomath.*, **11**(7):1850089, 2018, https://doi.org/10.1142/S1793524518500894.
19. N.C. Pati, G.C. Layek, N. Pal, Bifurcations and organized structures in a predator-prey model with hunting cooperation, *Chaos Solitons Fractals*, **140**:110184, 2020, https://doi.org/10.1016/j.chaos.2020.110184.
20. K. Sarkar, S. Khajanchi, Impact of fear effect on the growth of prey in a predator-prey interaction model, *Ecol. Complexity*, **42**:100826, 2020, https://doi.org/10.1016/j.ecocom.2020.100826.
21. L. Shi, J. Zhou, Y. Ye, Global stability and hopf bifurcation of networked respiratory disease model with delay, *Appl. Math. Lett.*, **151**:109000, 2024, https://doi.org/10.1016/j.aml.2024.109000.
22. P.A. Stephens, W.J. Sutherland, R.P. Freckleton, What is the Allee effect?, *Oikos*, **87**(1):185–190, 1999, https://doi.org/10.2307/3547011.
23. S.H. Streipert, G.S.K. Wolkowicz, M. Bohner, Derivation and analysis of a discrete predator–prey model, *Bull. Math. Biol.*, **8**:67, 2022, https://doi.org/10.1007/s11538-022-01016-4.
24. X. Wang, L. Zanette, X. Zou, Modeling the fear effect in predator–prey interactions, *J. Math. Biol.*, **73**:1179–1204, 2016, https://doi.org/10.1007/s00285-016-0989-1.
25. X. Wang, X. Zou, Modeling the fear effect in predator–prey interactions with adaptive avoidance of predators, *Bull. Math. Biol.*, **79**:1325–1359, 2017, https://doi.org/10.1007/s11538-017-0287-0.
26. Y. Ye, J. Zhou, Y. Zhao, Pattern formation in reaction-diffusion information propagation model on multiplex simplicial complexes, *Inf. Sci.*, **689**:121445, 2025, https://doi.org/10.1016/j.ins.2024.121445.
27. L.Y. Zanette, A.F. White, M.C. Allen, M. Clinchy, Perceived predation risk reduces the number of offspring songbirds produce per year, *Science*, **334**(6061):1398–1401, 2011, https://doi.org/10.1126/science.1210908.
28. J. Zhang, J. Su, Bifurcations in a predator–prey model of Leslie-type with simplified Holling type IV functional response, *Int. J. Bifurcation Chaos*, **31**(4):2150054, 2021, https://doi.org/10.1142/S0218127421500541.
29. J. Zhao, Complexity and chaos control in a discrete-time Lotka–Volterra predator–prey system, *J. Difference Equ. Appl.*, **26**(9–10):1303–1320, 2020, https://doi.org/10.1080/10236198.2020.1825702.
30. J. Zhou, Y. Ye, A. Arenas, S. Gómez, Y. Zhao, Pattern formation and bifurcation analysis of delay induced fractional-order epidemic spreading on networks, *Chaos Solitons Fractals*, **174**:113805, 2023, https://doi.org/10.1016/j.chaos.2023.113805.